

III-1

Accelerators and
Instruments

Development of 90° Bend-Type Spin-Rotator for Inverse Photoemission Spectroscopy

Y. Kajiura¹, T. Inagaki^{1,3}, N. Yamamoto^{1,2}, M. Hosaka², A. Mano²,
Y. Takashima^{1,2}, T. Konomi³ and M. Katoh^{2,3}

¹ Graduate School of Engineering, Nagoya University, Nagoya, 464-8603

² Nagoya University Synchrotron Radiation Research Center, Nagoya, 464-8603

³ UVSOR Facility, Institute for Molecular Science (IMS), Okazaki, 444-8585

Transmission type (NEA-GaAs) spin-polarized electron sources, in which pump laser light is injected from the backside of the photocathodes and the polarized beam is extracted from the front side, have been developed. By using this type of photocathodes, the high brightness of $\sim 2 \times 10^7 \text{ A}\cdot\text{cm}^{-2}\cdot\text{sr}^{-1}$ and the high polarization of $\sim 90\%$ were achieved [1, 2].

At UVSOR, we are planning to apply this type of photocathodes to the Spin-resolved Inverse Photoemission Spectroscopy. For this purpose, a compact spin rotator is needed. A spin rotator enables us to obtain arbitrary direction of electron spin. Furthermore, to suppress the degradation of beam qualities, a compact (shorter length) electron transfer system is essential. Therefore, we have designed and manufactured a compact spin rotator combined with the 90° bending function.

Arbitrary spin direction according to the beam direction is obtained by applying magnetic and electric forces simultaneously [3]. The designed spin rotator consists of in-situ spherical electrodes (curvature radius of 50mm and electric poles gap of 5mm), and a C-type bending magnet. We have designed the electro and magnetic components based on numerical calculations by using the Poisson code (2D) and Radia code (3D) [4]. The beam trajectories were also evaluated by using the GPT code.

From the electrode structure described above, the curvature radius of 50 mm and magnetic pole gap of $> 48 \text{ mm}$ were required for the bending magnet. Because the beam trajectories evaluated by using only electric or magnetic field should be equal and the vacuum chamber should be placed in the space between the magnet and the electrodes. In the simple C-type magnet case, it is difficult to satisfy the requirement for beam curvature due to the fringing field. Then we have employed two sets of return yoke and shield pole for both inject and extract sides.

As the result of the design, the spin-rotator size was decided 198mm x 175mm x 130 mm (W, D, H). Based on the numerical designs, we manufactured the bending magnet and the vacuum chamber (Fig.1). The magnetic coil parameters were decided in the consideration of wire-heating and current accuracy. The coil consists of 30-turns electric wires and the operation current is calculated to be around 7A.

Figure 2 shows the measurement field values and it is found that the result can be reproduced the numerical calculation values with sufficient accuracy.

The beam trajectories were also evaluated from various designed fields. In the case that only the magnetic field is applied, which corresponds to the parallel spin direction mode, the maximum beam discrepancy between obtained and ideal trajectories was obtained and estimated to be + 1.04 mm. Because the acceptable discrepancy for beam transfer is $\pm 1.8 \text{ mm}$, it is confirmed that the designed spin rotator has sufficient performance.

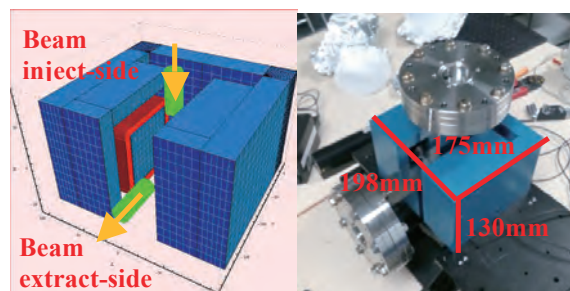


Fig. 1. 3D analysis model and fabricated spin rotator

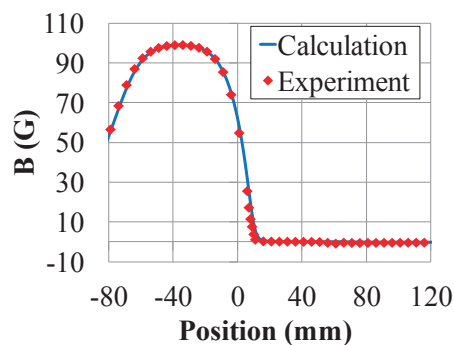


Fig. 2. Result of magnetic field measurement.

[1] N. Yamamoto, T. Nakanishi *et al.*, J. Appl. Phys. **103** (2008) 064905.

[2] X. G. Jin, N. Yamamoto *et al.*, Appl. Phys. Ex. **1** (2008) 045002.

[3] Andersen W. H. J., J. Appl. Phys. **18** (1967)1573.

[4] RADIA_URL:

“<http://www.esrf.fr/machine/support/ids/Public/Codes/software.html>”

Study on Vacuum Ultraviolet Coherent Harmonic Generation Using Relativistic Electron Beam and Laser

S. Sekita¹, M. Hosaka², N. Yamamoto^{1,2}, Y. Takashima^{1,2},
K. Hayashi³, J. Yamazaki³, T. Konomi³ and M. Katoh³

¹Graduate School of Engineering, Nagoya University, Nagoya 464-8603, Japan

²Nagoya University Synchrotron Radiation Research Center, Nagoya 464-8603, Japan

³UVSOR, Institute for Molecular Science, Myodaiji-cho, Okazaki 444-8585, Japan

At UVSOR-III, we are developing a coherent VUV light source using coherent harmonic generation (CHG) technique. An optical klystron, consisting of two Apple-II type undulators and an electro-magnetic buncher, has been already installed in BL1U. Recently, we installed a VUV spectrometer at the U1 experimental end station and made a CHG experiment. Figure 1 shows a schematic diagram of the measurement system including the spectrometer and figure 2 shows a photograph of the actual system.

In the experiment, we employ Ti:Sa laser with 800 nm wavelength and 100 fsec pulse width as a seed light source and observe 3rd-CHG (266 nm) using the spectrometer. Figure 3 shows the measured CHG spectrum.

The measured spectral width is 2.2 nm and assuming Fourier-transform-limited pulse the pulse duration is 50 fs. The value is shorter than the incident laser pulse width. Measured CHG intensity is 30 times of the SR intensity (Fig. 4), however the value is weaker than that of the calculated one [1]. This suggests that the interaction with the laser takes place not in the whole bunch but only limited transverse region due to poor alignment between the laser and the electron bunch. In the near future, we are going to install an improved laser alignment system.

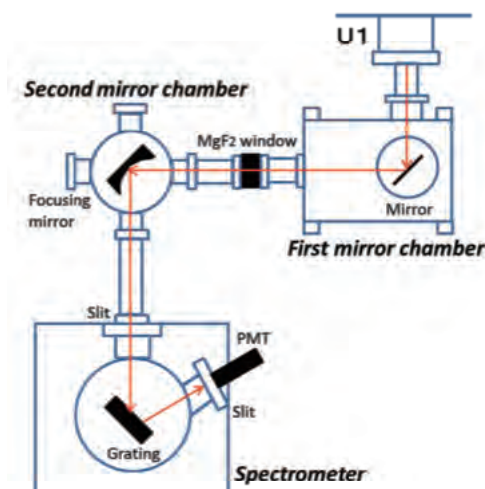


Fig. 1. Schematic of the measurement system for the CHG experiment.

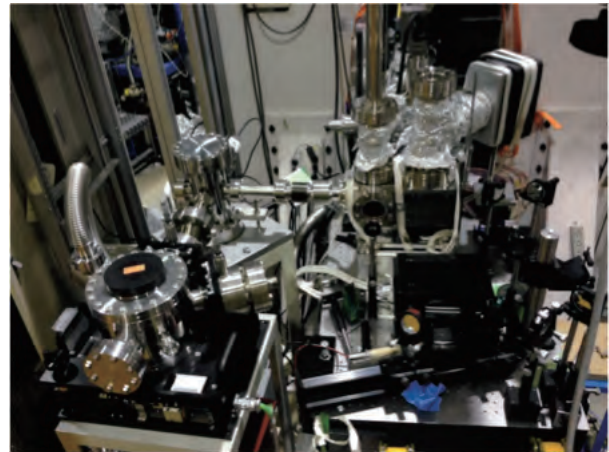


Fig. 2. Photograph of the measurement system.

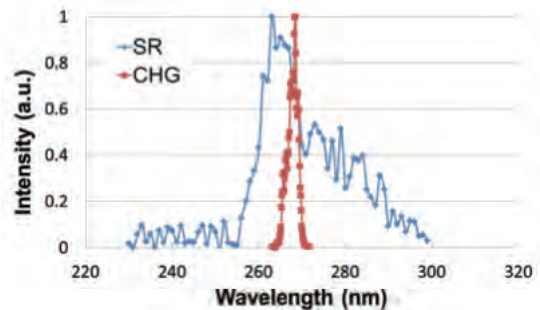


Fig. 3. Observed 3rd-CHG spectrum compared with spontaneous synchrotron radiation.

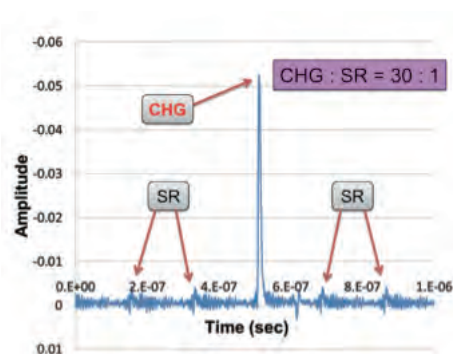


Fig. 4. Observed CHG radiation intensity

[1] S. Sekita, Master's Thesis, Nagoya University (2014).

Development of Deep Ultraviolet Pulse Compressor for Coherent Harmonic Generation Experiments

H. Zen¹, T. Konomi^{2,3} and M. Katoh^{2,3}

¹Institute of Advanced Energy, Kyoto University, Uji 611-0011, Japan

²UVSOR Facility, Institute for Molecular Science, Okazaki 444-8585, Japan

³The Graduate University for Advanced Studies (SOKENDAI), Okazaki 444-8585, Japan

The Coherent Harmonic Generation (CHG) from relativistic electron beam through the Free Electron Laser (FEL) interaction with high power laser is promising way to generate short pulse EUV coherent radiation [1]. However, power saturation occurs when the incident laser pulse is too strong and it limits the number of photon in a pulse [2]. In conventional laser, Chirped Pulse Amplification (CPA) technique is commonly used for avoiding damage or power saturation and to obtain high output power. We proposed utilization of CPA to CHG technique to overcome the saturation problem [3].

We are planning to make proof of principle experiment at the wavelength of 266 nm, the 3rd harmonics of Ti-sapphire laser. For the experiment, we need a pulse duration measurement system and a DUV pulse compressor.

In this fiscal year, we have constructed a DUV pulse compressor. The schematic diagram is shown in Fig. 1. The pulse compressor consists of a DUV grating, a periscope, 500-mm linear translation stage, a roof mirror and dielectric mirrors. The group velocity dispersion (i.e. compression factor) of this compressor can be controlled by changing the position of roof mirror. Figure 2 shows the photograph of the developed compressor. In this compressor, DUV laser pulse experiences four times diffraction on the same grating.

In order to adjust the compressor and check the efficiency, DUV laser pulses ($\lambda = 266$ nm) are generated by 3rd harmonic generation of Ti-Sapphire laser using 2nd and 3rd harmonic generation crystals. After finishing the adjustment of compressor, the incident and transmitted DUV laser power were

measured by a power meter (PH10I-Si-USB). As the result, the measured incident power was 470 μ W and transmitted power was 120 nW. The measured efficiency or transmittance of the compressor was 2.6×10^{-4} and calculated diffraction efficiency of the grating was around 13%. The diffraction efficiency of the grating measured in manufacturer at 300 nm and Littrow configuration was around 65%. The measured diffraction efficiency was significantly lower than that. We are planning to make further investigation on the polarization and incident angle dependence of diffraction efficiency to achieve higher transmission.

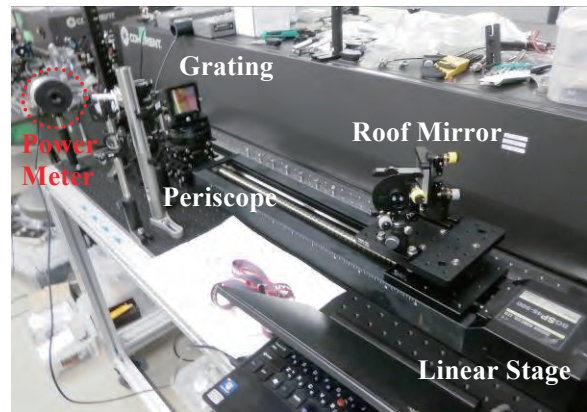


Fig. 2. Photograph of the developed pulse compressor

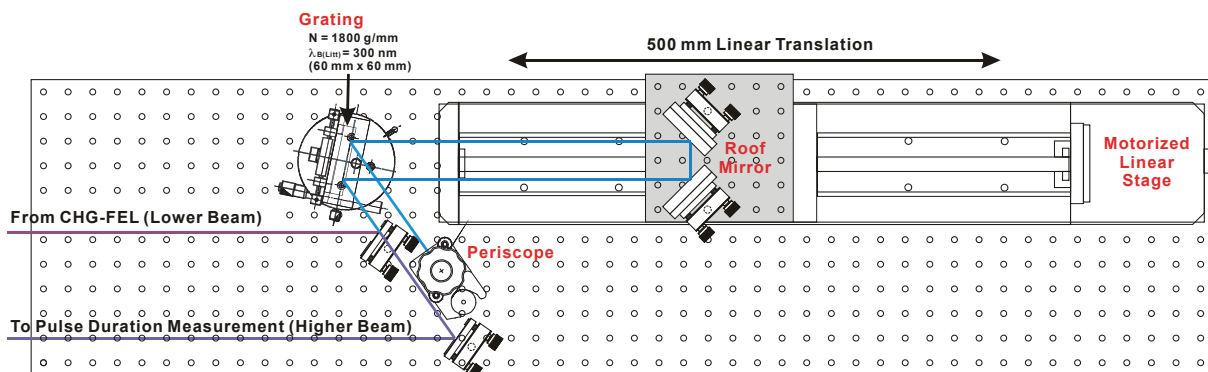


Fig. 1. Schematic drawing of pulse compressor.

[1] R. Prazeres *et al.*, Nucl. Inst. Meth. A **304** (1991) 72-76.

[2] T. Tanikawa *et al.*, Appl. Phys. Exp. **3** (2010) 2702.

[3] H. Zen *et al.*, Proc. of FEL2011 (2012) 366-369.

Others

Performance Evaluation of New Type Nuclear Emulsion with Electron Beam

K. Ozaki¹, S. Aoki¹, K. Kamada¹, E. Shibayama¹, S. Takahashi¹, S. Tawa¹, F. Mizutani¹,
H. Kawahara², H. Rokujo² and GRAINE collaboration

¹Department of Human Environment Science, Kobe University, Kobe 657-8501, Japan

²Graduate School of Science, Nagoya University, Nagoya, 464-8602, Japan

We are promoting GRAINE project [1], which is balloon-borne experiment to explore the gamma-ray astrophysics with nuclear emulsion.

Nuclear emulsion is a 3-dimensional tracking detector with 0.1 μm precise position resolution. Nuclear emulsion records the track of silver grains produced by trajectory of charged particle (see Fig. 1). Self-production of new type emulsion has developed at Nagoya University since 2010. The performance evaluation of new type emulsion is presented. This work is mainly for next balloon experiment of GRAINE in 2014, Australia.

In order to control / improve the sensitivity to the charged particle, four types of emulsions which are changed the amount of silver halide were developed at Nagoya University. Emulsion films were made by coating emulsion on both side of plastic base. These films were exposed to electron beam at UVSOR to evaluate their sensitivity. After development the films, the measurement of the numbers of silver grains was done with optical microscope.

Figure 2 shows the result of measurement of Grain Density (GD: counts of silver grains per 100 μm) for four types of emulsions. Development time is 25 minutes for all types. There is good correlation between GD and the amount of silver halide. GD of conventional nuclear emulsion (OPERA film [2]) is about 30, so we could succeed to improve the sensitivity by increasing the amount of silver halide. While multiple coulomb scattering increases due to the increasing the amount of silver halide, so there is trade-off.

It is also important to evaluate about characteristic of long-term preservation of new type emulsion film. In the case of GRAINE, it takes about 6 months from film production to balloon flight. This time we have evaluated about the highest silver halide type of emulsion. Films were exposed to electron beam at UVSOR just after production, and 1, 2.4, 3.8, 4.9 months after production. Preservation environment is shielded place with lead block at room temperature and humidity (about 14-20 degree and 40-60 %RH). After development the films, the measurement of GD was done with optical microscope.

Figure 3 shows the result of long-term preservation of new type emulsion film. Development time is 20 minutes mainly, but film of 3.8 months after is 25 minutes. Black and red circle means difference of measurement person. GD is almost stable after 5months. There is no problem about characteristic of

long-term preservation to perform the GRAINE and other experiments.

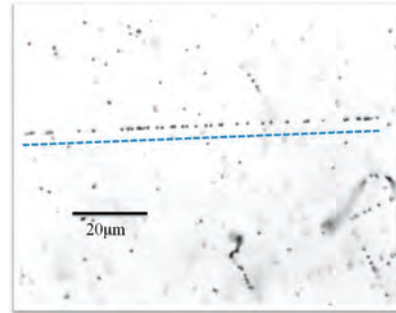


Fig. 1. Microscopic view of emulsion recorded charged track.

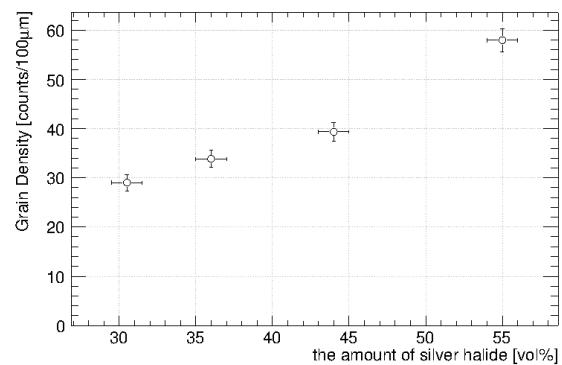


Fig. 2. The amount of silver halide dependence of Grain Density.

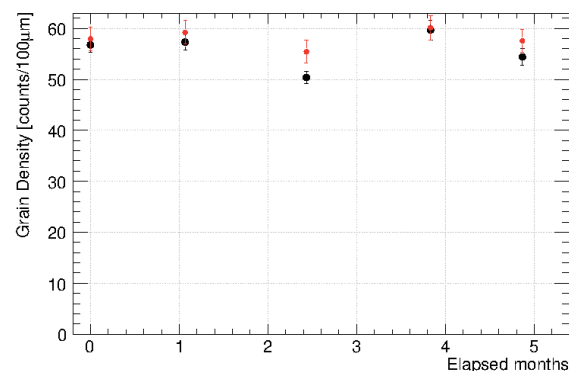


Fig. 3. Characteristic of long-term preservation of new type emulsion film.

- [1] S. Aoki *et al.*, <arXiv: 1202. 2529 [astro-ph.IM]>.
[2] T. Nakamura *et al.*, Nucl. Instr. Meth. A **556** (2006) 80.

BL2B

Reconstruction of the Beamline BL2B for Development of Photoelectron Spectroscopy for Organic Materials

S. Kera¹, K. R. Koswattage^{1,2}, K. Yonezawa¹, J. P. Yang¹, Y. Nakayama¹, K. K. Okudaira¹ and H. Ishii¹

¹ Graduate School of Advanced Integration Science, Chiba 263-8522, Japan

² UVSOR Facility, Institute for Molecular Science, Okazaki 444-8585, Japan

Electronic/optical devices based on π -conjugated molecular semiconductors have moved out of the field of the academic curiosity and are now regarded as valuable brilliant technologies as found for organic field-effect transistors and organic photovoltaics etc. However the fundamental pictures of the intrinsic electronic and optical properties are often hindered by the presence of chemical and physical imperfections, eg. chemical impurities, energetic and structural disorder. Thus, the development in the surface science technique and the availability of research stations at synchrotron facility suited for characterizing the wide range of molecular materials is desired for achieving the fundamental understanding.

The bending-magnet beamline of BL2B is developed by Prof. Mitsuke *et al.*[1,2], where the 18-m spherical grating monochromator (Dragon type) with three gratings (G1 – G3) and four mirrors (M1 – M4) to achieve a high-resolution and photon flux and had been used for gas-phase experiments. The monochromator can cover the energy range of 23-205 eV, a resolving power of 2,000-8,000 and photon flux of more than 10^{10} photons/s[2].

We started the reconstruction of the beamline for photoelectron spectroscopy of molecular solids in September 2013. In the monochromator, it is necessary to insert two plane mirrors M2 and M3 across the photon-beam between G3 grating and S2 slit in order to get precious light from G3 grating. These mirrors should be removed from the optical path when G1 or G2 grating is employed. However, there was a problem of the linear motion of the mirror system due to a deformation of a vacuum rod in between mirror and motor system. A new vacuum rod has been replaced (TOYAMA) in order to solve the malfunction of the M2 and M3 mirror system.

A UHV chamber *so called* monitoring chamber has been placed downstream of the refocusing mirror chamber. The monitoring chamber contains three linear motion feedthroughs, where a silicon photodiode for absolute photon flux measurement (AXUV-100, IRD), a sapphire plate to monitor the photon-beam position, a Au mesh of the size 100 to monitor the relative photon flux and for the beamline alignment. The third feedthrough is to equip the filters to attenuate higher order light and, at the present foil structure of Al/Mg/Al filter (LUXEL) is attached. The same chamber can be also employed for gold evaporation.

A new interlock system has been introduced to ensure the safety of users as well as prevent damage

to the beamline and storage ring in case of accidents. The safety interlocks at six vacuum valves of the beam line are controlled by a system with vacuum gauge readings. There is a touch-panel display and the screen show a schematic drawing of the beamline along with vacuum valve status. Further, two power distribution units have been built for proper handling the electricity in the beam line.

A new end-station for the photoelectron spectroscopy equipped with a hemispherical analyzer (SCIENIA R3000) and a liquid-He-cooled cryostat (temperature range of 15-400 K) with 5-axis stage is transferred from Chiba Univ. The experimental chambers have been adjusted to place for the photon-beam trajectory.

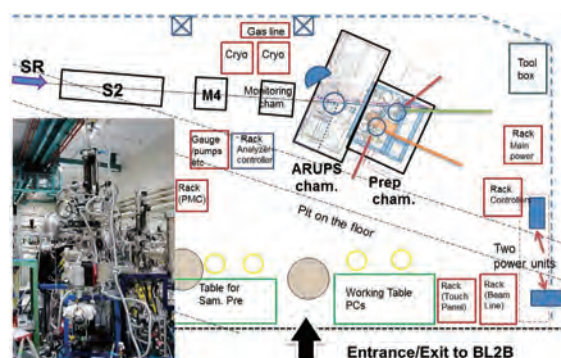
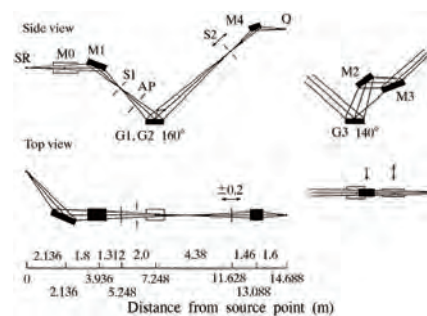


Fig. 1. (top) BL2B equipped with an 18-m SGM. Two optical paths with including angles of 160° for G1 and G2 and 140° for G3 are indicated. S2: exit slit; Q: sample point (after ref [1]). (bottom) Schematic layout of BL2B.

[1] H. Yoshida and K. Mitsuke, *J. Synch. Rad.* **5** (1998) 774.

[2] M. Ono, H. Yoshida and K. Mitsuke, *Nucl. Instrum. Meth. Phys. Res. A* **467-468** (2001) 577.

BL3B

Observation of VUV Emission from Al_2O_3 and $\text{Nd}:\text{LaF}_3$ Crystals

M. Kitaura¹, S. Kurosawa^{2,3}, J. Pejchal², K. Fukui⁴, K. Nakagawa⁵, S. Watanabe⁶,
A. Ohnishi¹, K. Ogasawara⁶, M. Hasumoto⁷ and M. Sakai⁷

¹Department of Physics, Faculty of Science, Yamagata University, Yamagata 990-8560, Japan

²Institute for Materials Research, Tohoku University, Sendai 980-8679, Japan

³New Industry Creation Hatchery Center, Tohoku University, Sendai 980-8679, Japan

⁴Department of Electrical and Electronics Engineering, University of Fukui, Fukui 910-8507, Japan

⁵Graduate School of Human Development and Environment, Kobe University, Kobe 657-8501, Japan

⁶School of Science and Technology, Kuwansei University, Sanda 669-1337, Japan

⁷UVSOR facility, Institute for Molecular Science, Okazaki 444-8585, Japan

Since 2011, the BL3B beamline offers many researchers for the opportunity of spectroscopy experiment using VIS, UV and VUV photons to many researcher [1]. One of the next targets is to extent observable emission range to higher-energy side. Few VUV emission spectroscopic experiments have been performed in synchrotron radiation facilities. The SUPERLUMI station at HASYLAB in DESY was the only experimental setup for VUV emission spectroscopy; however, it still remains closed at present. We have installed the spectroscopy system consisting of two MgF_2 lenses, a CCD detector (Princeton Instruments SX-100B) and a monochromator (Acton VM-502) at the BL3B. To check whether this system works, we have measured VUV emission and excitation spectra of Al_2O_3 and Nd^{3+} -doped LaF_3 ($\text{Nd}:\text{LaF}_3$) crystals at 9 K. These crystals have been known to show VUV emission at low temperatures [2, 3].

Figure 1 shows the emission and excitation spectra of pure Al_2O_3 crystals. Blue squares clearly show that an emission band appears around 7.51 eV under excitation at 8.92 eV. This band is excited in the fundamental absorption band of Al_2O_3 . These data are in agreement with those published previously [2], where the 7.51 eV band was attributed to the radiative annihilation of self-trapped excitons (STEs).

Emission and excitation spectra of $\text{Nd}:\text{LaF}_3$ crystals are shown in Fig. 2. As indicated by blue squares, a sharp emission peak is observed around 7.08 eV under excitation at 7.75 eV. The 7.08 eV band is excited in the $4f \rightarrow 5d$ absorption region of Nd^{3+} ions (red squares). This feature suggests that the 7.08 eV band is assigned to the $5d \rightarrow 4f$ transition of Nd^{3+} ions. The observed spectra are almost the same as those in Ref [3]. Another band is seen around 5.74 eV, also being assigned to the $5d \rightarrow 4f$ transition of Nd^{3+} ions.

We will install a focus mirror system the nex year to collect VUV emission more efficiently next year. This is vital for the detection of VUV emission, because the sensitivity of the detector such as PMT and CCD is relatively low in the VUV range. Furthermore, the experimental setup for the time-resolved emission and excitation spectroscopy in the wide energy range from VIS to VUV will be also

installed for the investigation of photo-excited state dynamics in crystalline solids.

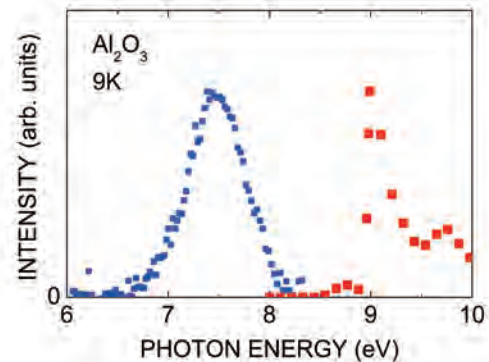


Fig. 1. Emission (blue) and excitation spectra (red) for the Al_2O_3 crystal. The emission and excitation spectra were measured at 9K for 8.92 eV excitation and 7.51 eV emission.

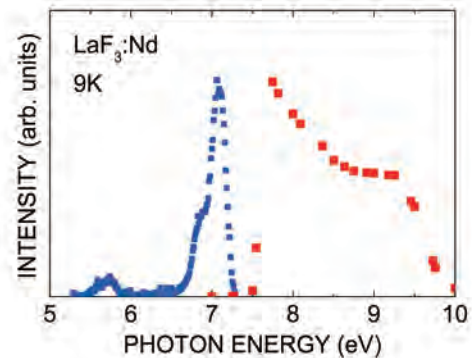


Fig. 2. Emission (blue) and excitation spectra (red) for the Nd^{3+} -doped LaF_3 crystal. The emission and excitation spectra were measured at 9K for 7.75 eV excitation and 7.08 eV emission.

[1] K. Fukui *et al.*, *J. Synchrotron Rad.* **21** (2014) 452.

[2] V. V. Harutunyan *et al.*, *Eur. Phys. J. B* **12** (1999) 35.

[3] P. Dorenbos *et al.*, *J. Lumin* **69** (1996) 229.

BL7B

Stokes Parameters Measured by VUV Spectral Ellipsometer

T. Saito¹, K. Ozaki² and K. Fukui²¹Faculty of Engineering, Tohoku Inst. Tech., Sendai 982-8577, Japan²Faculty of Engineering, Univ. of Fukui, Fukui 910-8507, Japan

Ellipsometers are known as powerful tools to determine optical properties such as optical constants of thin films or bulk materials [1]. For typical ellipsometers, the photon beam entering the sample should be highly polarized or its polarization state should be characterized. Contrary to typical ellipsometers, the one developed [2] is capable to determine the photon source Stokes parameters as well as the sample optical constants.

Figure 1 shows a schematic structure of the VUV ellipsometer. Monochromatic radiation hits a sample at an angle of incidence of 67.5° or 45° . The reflected beam is detected with an inclined photodiode with an angle of incidence of about 40° . The ellipsometer chamber can be rotated around the axis of the incidence with angle α using a rotational feedthrough with magnetic sealing fluid. The analyzer unit can also be rotated around the reflected beam from a sample with angle β . Intensity measurements in the several combinations of α and β make it possible to analytically solve all the unknown parameters, that is, the Stokes parameters of the incident radiation, optical constants of the sample and detector polarization characteristics of the detector.

We used the ellipsometer at the normal incidence monochromator beamline, BL7B at UVSOR for three sample mirrors, Au, AlN and AlN photodiode. Complex refractive indices of AlN obtained were published elsewhere [3-4]. Figure 2 shows Stokes parameters obtained for the radiation emerging from BL7B. Note that measurements were repeated three times for each sample incidence angles of 45° and 67.5° by changing the sample mirrors. Although the data of S_2 and S_3 are somehow scattered, the data of S_1 shows better reproducibility independent of the sample mirror.

Considering the rather large vertical accepting angle, the results obtained are considered to be reasonable. It should be also mentioned that the polarization, in principle, could be different depending on the electron beam condition such as beam position and beam emittance in the storage ring. Although we were not able to attribute the cause of the scatter of S_2 and S_3 , it can be probable that the electron beam instability of the storage ring and/or difference in illuminating condition in the beamline optics is partly responsible for it since we observed rather big changes in Stokes parameters over many times measurements.

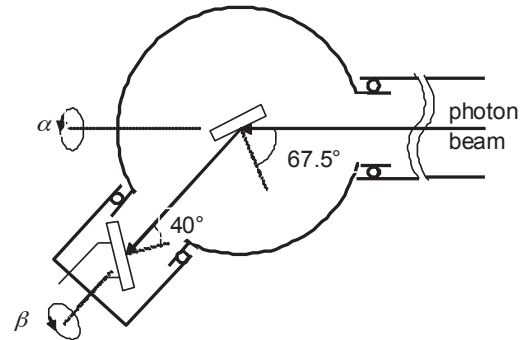
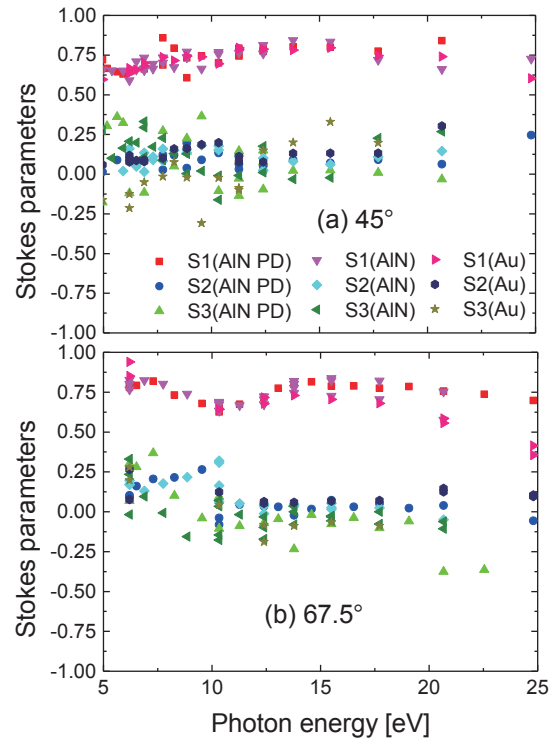


Fig. 1. Schematic layout of the ellipsometer.

Fig. 2. Stokes parameters obtained by the ellipsometer using 3 different samples. The angle of incidence to the sample: (a) 45° and (b) 67.5° .

[1] D. E. Aspnes, in: E. D. Palik (Ed.), *Handbook of Optical Constants of Solids* (Academic Press, Boston, 1985).

[2] T. Saito, M. Yuri and H. Onuki, *Rev. Sci. Instrum.* **66** (1995) 1570.

[3] K. Ozaki *et al.*, *UVSOR Activity Report* **38** (2010) 105.

[4] T. Saito *et al.*, *Thin Solid Films*, available online 12 March 2014

(<http://dx.doi.org/10.1016/j.tsf.2014.02.099>).

BL7B

Efficiency Measurement of a Holographic Concave Grating for VUV Solar Spectro-Polarimetry

H. Hara^{1,2}, M. Kasuga², T. Kobiki¹, K. Miyagawa² and N. Narukage³

¹National Astronomical Observatory of Japan, Mitaka 181-8588, Japan

²Department of Astronomy, School of Science, The University of Tokyo, Tokyo, 113-0033 Japan

³Institute of Space and Astronautical Science, JAXA, Sagami-hara, 252-5210, Japan

We are developing a payload of a sounding rocket experiment named the Chromospheric Lyman-Alpha Spectro-Polarimeter (CLASP) [1] (Fig. 1). CLASP is an instrument to detect low-level polarization signals with an order of 0.1% photometric sensitivity in the H Lyman-alpha line at 121.6 nm for the measurement of magnetic fields in the upper chromosphere and transition region of the Sun. A holographic-ruled spherical concave grating of 110 mm diameter with a 3000 gr/mm groove density is used in the spectro-polarimeter that requires a high efficiency (>0.18). The grating for the experiment was fabricated by Horiba Jobin Yvon (HJY), which has rich heritages for providing the flight gratings in the space programs.

In parallel with developing the flight optics, we have been developing the grating for the future use in space astronomy with domestic companies. One of the programs is to make a high-efficiency holographic concave grating in collaboration with Shimadzu Corporation. The grating specification is almost the same as that of the CLASP flight grating. It has a spherical concave surface of 110mm effective area with groove density of 3,000 gr/mm and a rectangular groove shape reshaped by the ion-beam etching process. Three gratings fabricated this time are master gratings. The grating substrate is fused silica, while Zerodur is used for the CLASP replica gratings. Al/MgF₂ is coated on the grating surface to enhance the diffraction efficiency.

Figure 3 shows the absolute grating efficiency of one of three gratings measured at the beam line BL7B. Although non-uniformity in efficiency is found over the effective grating aperture, the efficiency is good enough for the specification for the CLASP grating, and is comparable to the CLASP flight gratings that have been fabricated by HJY. The reflectance of the witness sample mirror coated by Al/MgF₂ with the concave grating is 0.75 at 121nm, so that the 30–40% groove efficiency has been achieved. Other two gratings have also shown good absolute efficiency of 0.24-0.28 with better uniformity over the grating surface, though they partially have areas with low efficiency of 0.05 due to the local failure of groove formation.

This work was supported by a Grant-in-Aid for Scientific Research (B) (No. 23340052) from the

Ministry of Education, Culture, Sports, Science and Technology of Japan.



Fig. 1. Concave grating in the CLASP polarimeter.

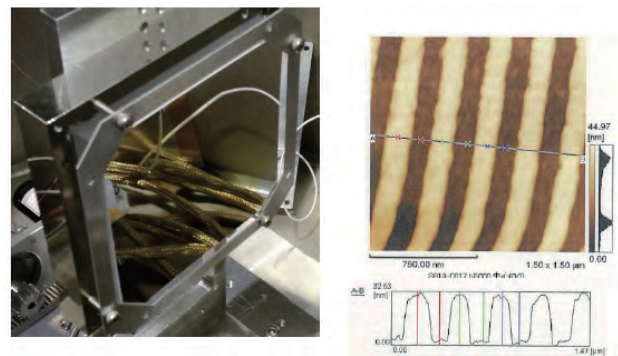


Fig. 2. (left) Holographic spherical concave grating fabricated by Shimadzu Corporation and (right) its groove profile.

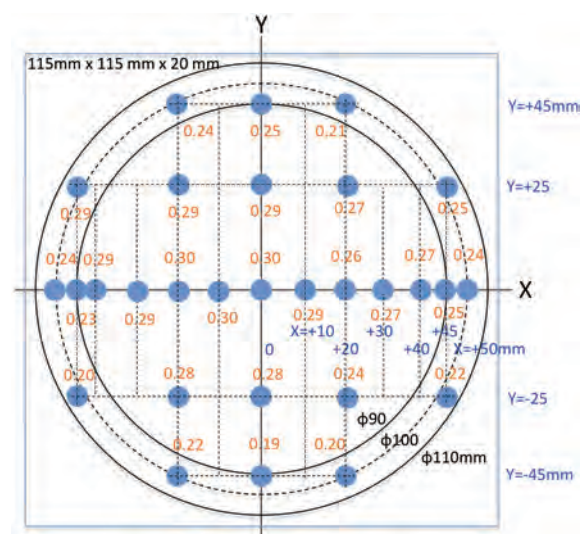


Fig. 3. Absolute grating efficiency of the holographic concave grating measured at 121nm in red characters.

[1] R. Kano *et al.*, SPIE **8443** (2012) 84434F.

BL7B

Performance Verification of Flight Filter Unit for CLASP Slit-Jaw System

M. Kubo¹, N. Narukage¹, G. Giono², R. Ishikawa¹, S. Ishikawa¹, K. Aoki³, T. Kobiki¹,
Y. Suematsu¹, T. Bando¹ and R. Kano¹

¹National Astronomical Observatory of Japan, Tokyo 181-8588, Japan

²Department of Astronomical Science, Graduate University for Advanced Studies (SOKENDAI), Tokyo 181-8585, Japan

³Department of Astronomy, University of Tokyo, Tokyo 113-0033, Japan

CLASP is a sounding rocket program, for the first time, to detect the linear polarization signal in Lyman alpha (121.567nm) emitted from the upper chromosphere or transition region of the Sun [1]. The telescope of CLASP focuses a solar image on a slit, and the light passing through the slit feeds into the spectropolarimeter that measures the spectra of the linear polarization. The outside of the slit has a mirror surface, and the solar image outside the slit is reflected to the slit-jaw system. The slit-jaw system will obtain Ly-alpha images by focusing optics with a pair of Ly-alpha narrow band filters. The images are used to select the instrument pointing during flight and to help the interpretation of the data obtained by the spectropolarimeter.

A filter unit (Fig.1) of the slit-jaw system holds a pair of Ly-alpha filters. The Ly-alpha filters are developed by the Acton Optics & Coatings. The diameter of the filter is one inch and its thickness is 2.5mm. The filter unit is fabricated by the Genesis Corporation. Their designs are based on measurements of prototype of Ly-alpha filters in FY2011 [2].

The transmissivity in Ly-alpha and the visible light rejection performance of the Ly-alpha filters are important for obtaining Ly-alpha images because the amount of photons in the visible light is much higher than photons in Ly-alpha wavelength. Figure 2 shows the transmissivity of a witness sample that is coated simultaneously with the flight Ly-alpha filters. The transmissivity is 10% in the Ly-alpha wavelength and less than 10^{-3} % for the visible light. The measured transmissivity satisfies our requirements, and then the visible light contamination is less than 1% in the Ly-alpha images. We conclude that the flight Ly-alpha filters are successfully fabricated.

A pair of Ly-alpha filters is mounted at the angle of incidence (AOI) of 0 degree, and the coated surfaces of the two filters face each other at a distance of 5mm. The ghost images are created by the reflection on the back and coated surfaces of a filter, and by the reflection between two filters. The Ly-alpha images though the flight filter unit are taken by CCD camera at AOI = 0 and AOI= ± 10 degrees (Fig.3). We have confirmed no issue of the ghost images created by the filter unit: (1) the intensity of ghost beams to the main beam is less 1%, (2) the distance between the ghost beam and main beam is expected value (about 1.7mm

in the case of AOI= ± 10 degree), and (3) there is no unexpected ghost pattern.

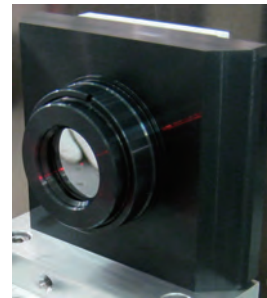


Fig. 1. Photo of the CLASP filter unit.

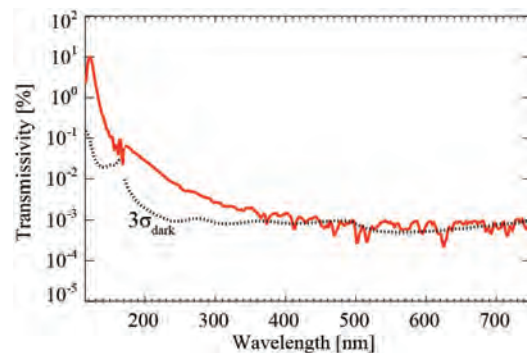


Fig. 2. Transmissivity of the Ly-alpha filter (red line).

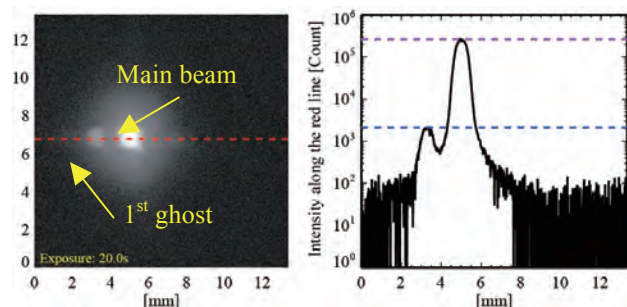


Fig. 3. *Left:* Main beam and ghost beam image created by the filter unit at the AOI of 10 degree. *Right:* Intensity along the dashed red line in the left panel.

[1] R. Kano *et al.*, SPIE **8443** (2012) 84434F.

[2] M. Kubo *et al.*, UVSOR Activity Report **39** (2011) 43.

BL7B

Waveplate Axis Alignment for the CLASP Sounding Rocket

S. Ishikawa¹, G. Giono², R. Ishikawa¹, N. Narukage¹, R. Kano¹ and T. Bando¹

¹National Astronomical Observatory of Japan, Tokyo 181-8588, Japan

²Department of Astronomical Science, Graduate University for Advanced Studies (SOKENDAI), Tokyo 181-8585, Japan

The Chromospheric Lyman-Alpha SpectroPolarimeter (CLASP) is a sounding rocket experiment to observe the linear polarization profile of the Lyman-alpha line (vacuum ultraviolet, 121.6 nm) from the Sun for the magnetic field measurement in the upper chromosphere and transition region [1]. CLASP uses a continuously rotating MgF₂ half-waveplate [2] and reflecting polarization analyzer to measure the Lyman-alpha linear polarization. A digital signal to trigger the CCD camera exposure is sent out from the motor every 22.5-degree rotation of the waveplate to drive the linear polarization degree and angle. To measure the polarization angle precisely, it is necessary to align the waveplate on the motor with a small angle uncertainty. The estimated polarization angle uncertainty from the CCD photon noise is 0.8-degree, and the goal was to align the waveplate with respect to the motor with better than 0.8-degree. Before this alignment experiment, the waveplate angle is adjusted just by looking at a reference marking-off on the waveplate edge by eye, and the uncertainty is not smaller than a few degrees.

We measured the relative angle between the waveplate and motor with the UVSOR BL7B beam with the wavelength of the Lyman-alpha light, and adjusted the waveplate angle. The experimental setup is shown in Fig. 1 and Fig. 2. We made the linearly polarized Lyman-alpha beam by the UVSOR beam with a reflecting polarization analyzer. The polarized beam is going through the rotating waveplate, and the polarization direction changes continuously. The linear polarization component parallel to the certain direction is extracted by the reflecting polarization analyzer and a time profile of the intensity of the extracted component is recorded by a photodiode. The recorded time profile, which is called the polarization modulation, and the exposure synchronization signal are recorded simultaneously. The rotation speed of the motor is 4.8 seconds per one rotation; therefore we measured the signals with the high sampling frequency of 1 kHz to estimate the waveplate angle with the better precision than 0.1-degree (one sampling interval of 1 ms corresponds to 0.075-degree).

We estimated the deviation angle of the waveplate with respect to the motor to be 0.66-degree from the obtained polarization modulation (shown in Fig. 3). We adjusted the waveplate angle to cancel the deviation. After the adjustment, we measured the polarization modulation and the exposure

synchronization signal again, and the deviation was ~0.05-degree. Therefore, we confirmed that the waveplate angle is successfully aligned and the remained deviation was much less than the requirement.

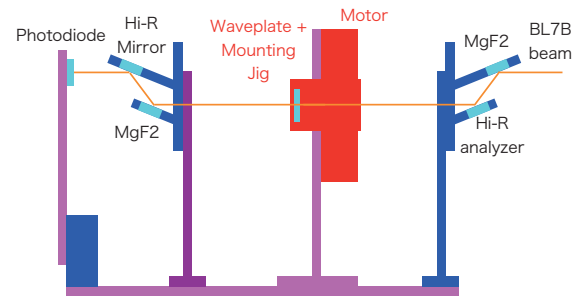


Fig. 1. Overview of the experimental setup.

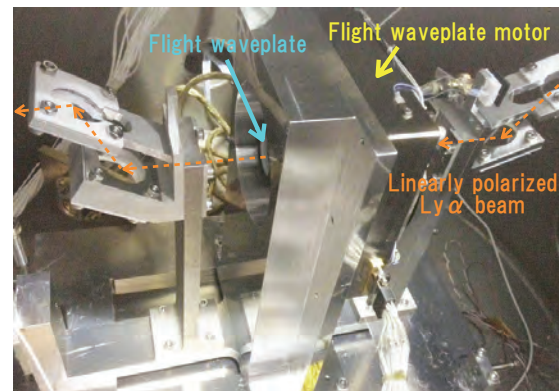


Fig. 2. Photo of the experimental setup.

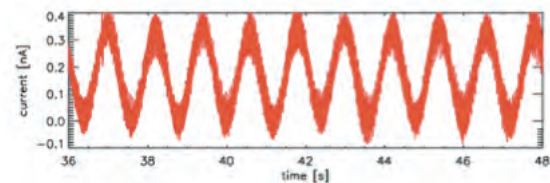


Fig. 3. Obtained polarization modulation. Only a part (10 seconds, ~2 waveplate rotation) of the obtained data is plotted.

[1] R. Kano *et al.*, SPIE **8443** (2012) 84434F.

[2] R. Ishikawa *et al.*, Appl. Optics. **52** (2013) 8205.

BL7B

Development of Mechanically Ruled Grating for the VUV Application

R. Ishikawa¹, S. Ishikawa¹, R. Kano¹, T. Bando¹, M. Koyama²,
Y. Enokida², T. Sukegawa³ and S. Tsuneta⁴

¹National Astronomical Observatory of Japan, Mitaka, 181-8588, Japan

²Corporate Production Engineering Headquarters, CANON Inc., Kawasaki, 212-8602, Japan

³Corporate R&D Headquarters, CANON Inc., Utsunomiya, 321-3292, Japan

⁴Institute of Space and Astronautical Science, Japan Aerospace Exploration Agency, Sagami-hara, 252-5210, Japan

For the vacuum-ultraviolet (VUV; $\lambda < 200\text{nm}$) applications, holographic gratings have been widely used, but here we focus on the capability of a mechanically ruled grating, since it is flexible in choice of groove density and surface figure compared with the holographic grating. As a first step of the development of a mechanically ruled VUV grating, we have fabricated a test sample made of NiP with the groove density of 5000 lines/mm and the effective area of 10 mm x 10 mm, and evaluated the performance at the UVSOR BL7B. Since we consider the possibility to apply this grating to the CLASP sounding rocket experiment [1] in the future, which intends to measure linear polarization at the hydrogen Lyman- α line (121.6 nm), our experiment was done with a focus on this wavelength. For the reference, we have also performed the measurement of the NiP plane mirror made by cutting work.

Figure 1 shows the photograph of the surface shape of the grating sample observed with the Atomic Force Microscope (AFM), and the micro-roughness is found to be very good with 0.6 nm RMS, indicating very low stray light. Figure 2 represents the reflectivity of 0th order with the angle of incidence (AOI) of 5 deg for TE (electric vector is parallel to the groove) and TM (electric vector is perpendicular to the groove). We found significant difference in the reflectivity between two incident polarization states; the reflectivity for TM is lower than that for TE, and the difference becomes larger at longer wavelength ($\lambda > 120\text{ nm}$). At the wavelengths of 183 nm and 217 nm (shown with dotted lines in Fig. 2), the TM reflectivity represents the local maximum, and these wavelengths correspond to the wavelengths, where +1st and -1st orders disappear for the grating with groove density of 5000 lines/mm at AOI=5deg. The diffraction efficiency of +1st and -1st orders at 121.6 nm is found to be 6.4% and 7.8% for TM and 11.0% and 12.1% for TE. The similarity in the reflectivity among +1st and -1st orders indicates that the groove shape is symmetrical, while the higher efficiency for TE indicates that the groove depth is not optimized for 121.6 nm (see next paragraph for more detail). We also find that the reflectivity of plane mirror sample at AOI=5deg is 28% at 121.6 nm. Thus, the relative diffraction efficiency of our grating sample is estimated to be 22 - 43%.

The measured reflectivity of the NiP plane mirror from 115 to 300 nm allows us to evaluate the optical constant of NiP and simulate the diffraction efficiency of the NiP grating. We found that the 0th order reflectivity and diffraction efficiency at +/-1st orders are consistent with the simulation results with the groove depth of 45 nm, and the groove depth of 28 nm gives us the well-balanced diffraction efficiency between TE and TM. We also found that the simulation depends strongly on the optical constant of the material, and the evaluation is necessary for the development of the grating.

The relative diffraction efficiency of our sample is large and reproduced by the simulation. The difference in efficiency between TE and TM, which should be avoided in the polarization measurement, can be suppressed by optimizing the groove depth. Thus, we conclude that the first step of the development of mechanically ruled gratings was successfully done. Next step is to develop the coating to enhance the absolute diffraction efficiency.

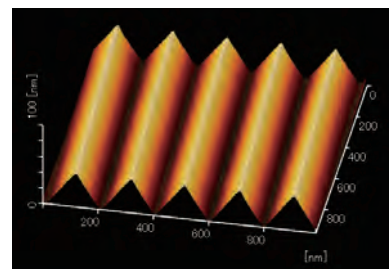


Fig. 1. Photo of grating surface.

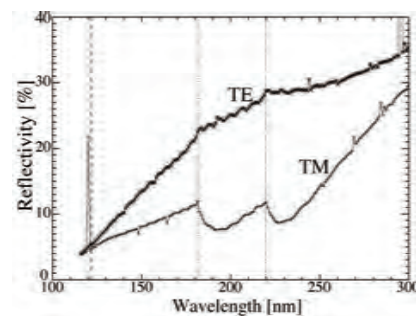


Fig. 2. Reflectivity of NiP grating sample at 0th order with AOI=5 deg for TE and TM.

[1] R. Kano *et al.*, SPIE **8443** (2012) 84434F.

BL7B

Birefringence of MgF₂ in the Vacuum Ultraviolet and Development of an MgF₂ Half-Waveplate

R. Ishikawa¹, R. Kano¹, T. Bando¹, Y. Suematsu¹, S. Ishikawa¹, Y. Katsukawa¹, M. Kubo¹, N. Narukage¹, H. Hara¹, S. Tsuneta², H. Watanabe³, K. Ichimoto⁴, K. Aoki⁵ and K. Miyagawa⁵

¹National Astronomical Observatory of Japan, Mitaka, 181-8588, Japan

²Institute of Space and Astronautical Science, Japan Aerospace Exploration Agency, Sagami-hara, 252-5210, Japan

³Unit of Synergetic Studies for Space, Kyoto University, Kyoto 607-8417, Japan

⁴Kwasan and Hida Observatories, Kyoto University, Takayama 506-1314, Japan

⁵Department of Astronomy, School of Science, The University of Tokyo, Tokyo 113-0033, Japan

Spectro-polarimetric observations in the vacuum-ultraviolet (VUV) region are expected to be developed as a new astrophysics diagnostic tool for investigating space plasmas with temperatures of $>10^4$ K. A team of researchers from Japan, the USA, Spain, France, and Norway has been developing the high-throughput chromospheric Lyman-alpha spectro-polarimeter (CLASP), which is aiming to measure the linear polarization of the hydrogen Lyman- α line ($\lambda = 121.567$ nm) for the first time [1]. Precise measurements of the difference in the extraordinary and ordinary refractive indices are required for developing accurate polarimeters, but reliable information on the birefringence in the VUV range is difficult to obtain. We have measured the birefringence of magnesium fluoride (MgF₂) around 121.57 nm at the BL7B beamline using prototype of MgF₂ waveplates, and developed a flight half-waveplate for the CLASP rocket experiment. Our waveplates consist of two stacked MgF₂ plates with slightly different thicknesses and their principal axes are rotated by 90° with respect to each other.

A schematic of our experimental setup is shown in Fig. 1. We employed three MgF₂ plates set at Brewster's angle (59°). Using two MgF₂ plates, linearly polarized light in the horizontal direction with a polarization degree of $>99.999\%$ was directed onto a waveplate sample. With this configuration, we measured the intensities I_{obs} at $\phi=0^\circ$ and $\phi=45^\circ$ (ϕ is the angle of the principle axis of a waveplate from the horizontal direction), and calculated the ratio which is a function of phase retardation δ , $A(\lambda)=I_{obs}(\phi=45^\circ)/I_{obs}(\phi=0^\circ)=[(1+PER)+(1-PER)\cos\delta(\lambda)]/2$. The polarization extinction ratio (PER) is the ratio of the p-polarization reflectivity to the s-polarization reflectivity. From the amplitude $A(\lambda)$, we determined δ as a function of wavelength and then derive the birefringence $n_e - n_o$ using $\delta = 2\pi(n_e - n_o)(d_1 - d_2)/\lambda$, where $d_1 - d_2$ is a thickness difference of two stacked MgF₂ waveplate. One of the difficulties in this measurement is the assignment of phase without 2π ambiguities. To achieve this, we measured several waveplate samples with different thickness differences (see [2] for more detail).

Figure 2 shows the birefringence of MgF₂ as a function of wavelength, derived from the phase retardation measurement of the waveplate sample with $d_1 - d_2 = 15.755$ μm . We found that $n_e - n_o = 0.004189 \pm 0.000039$ at 121.57 nm. Based on this birefringence, we fabricated the flight waveplate with $d_1 - d_2 = 14.51$ μm , and measured the phase retardation to be 2π at the BL7B. Thus, we conclude that we successfully completed the development of a half-waveplate for the CLASP experiment.

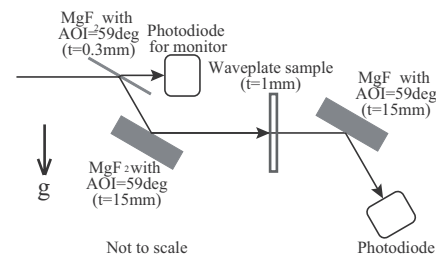


Fig. 1. Schematic of the experimental setup.

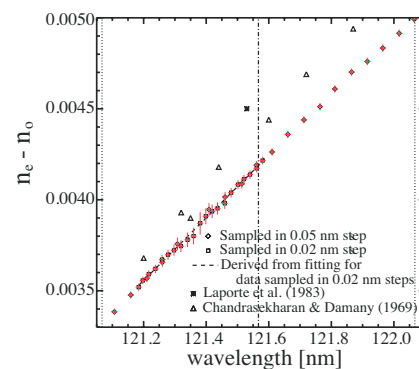


Fig. 2. Birefringence of MgF₂. Values measured in previous studies [3, 4] are also shown.

- [1] R. Kano *et al.*, SPIE **8443** (2012) 8443F.
- [2] R. Ishikawa *et al.*, Appl. Optics. **52** (2013) 8205.
- [3] V. Chandrasekharan and H. Damany, Appl. Opt. **8** (1969) 671.
- [4] P. Laporte *et al.*, J. Opt. Soc. Am. **73** (1983) 1062.

UVSOR User 2

